

Origin of Superconductivity in Boron-doped Diamond

K.-W. Lee and W. E. Pickett

Department of Physics, University of California, Davis, CA 95616

(Dated: September 5, 2018)

Superconductivity of boron-doped diamond, reported recently at $T_c=4$ K, is investigated exploiting its electronic and vibrational analogies to MgB_2 . The deformation potential of the hole states arising from the C-C bond stretch mode is 60% larger than the corresponding quantity in MgB_2 that drives its high T_c , leading to very large electron-phonon matrix elements. The calculated coupling strength $\lambda \approx 0.5$ leads to T_c in the 5-10 K range and makes phonon coupling the likely mechanism. Higher doping should increase T_c somewhat, but effects of three dimensionality primarily on the density of states keep doped diamond from having a T_c closer to that of MgB_2 .

PACS numbers: 71.20.-b, 71.20.Be, 71.20.Eh, 71.27.+a

Discovery of new types of superconducting materials has accelerated since the discovery of the high temperature superconductors, with a recent breakthrough being the discovery of superconductivity at $T_c=40$ K in the simple (structurally and electronically) compound MgB_2 . [1] The origin of its remarkable superconductivity is now understood to arise from charge carriers doped (in this case, self-doped) into very strongly bonding states that in turn respond very sensitively to the bond-stretching vibrational modes. [2] The strong B-B bonds in the graphitic layers of MgB_2 make it appear near optimal, although graphite itself and diamond are materials that have even stronger bonds. Of these two, only diamond has bonding states that can conceivably become conducting through hole-doping. [3] The recent report by Ekimov *et al.* [4] of superconductivity at 4 K in very heavily boron-doped diamond revives the question of mechanisms in strongly covalent materials. Confirmation has been provided by Takano *et al.* who report $T_c = 7$ K in B-doped diamond films. [5]

While the study of B as a hole dopant in diamond has a long history, there have been recent developments due to the ability to dope diamond films more heavily (to and beyond the 10^{20} cm^{-3} range) than was possible previously. In spite of its growing importance, and unlike the situation for donors, [6] there has been little theoretical work on the acceptor state (such as determining its spatial extent) beyond obtaining the structural and vibrational properties of the isolated B impurity. [7] An isolated B atom is an acceptor with a binding energy of 0.37 eV [8] for which effective mass theory is not applicable, but the behavior of B-doped diamond up to and somewhat beyond the concentration for insulator-metal (Mott) transition $c_M=2 \times 10^{20} \text{ cm}^{-3}$ has been rather well studied experimentally. [8] (The B concentration achieved by Ekimov *et al.* is about $c_{sc}=5 \times 10^{21} \text{ cm}^{-3} = 25c_M$, with a hole carrier density of nearly the same, and introduces a new regime of metal-

lic diamond that is yet to be understood.) At this concentration, B dopants are on average 5-6 Å apart and their donor states, which form an impurity band already at $c_M = \frac{1}{25}c_{sc}$, broaden considerably and overlap the valence band edge. In addition, Mamin and Inushima have pointed out [9] that as the B concentration increases (and they were not yet thinking of the 10^{21} range) many of the donor states become more weakly bound states of B-related complexes that would encourage formation of broader bands. Fontaine has analyzed the concentration dependence of the activation energy [10] (0.37 eV at low concentration) and concluded that it vanishes at $c = 8 \times 10^{20} \text{ cm}^{-3} = \frac{1}{6}c_{sc}$; for larger concentrations the system would be a degenerate metal.

Given these indications of degenerate behavior even below 2.5% doping, in this paper we adopt the viewpoint that the majority fraction of the hole carriers resides in states overlapping the diamond valence band, and behave primarily as degenerate valence band holes. Boeri *et al.* [11] have taken a similar viewpoint, and two supercell calculations [12, 13] have verified this degenerate metal picture. The distinctly different low-concentration, nonmetallic limit has also been suggested. [14] We investigate the magnitude and effect of hole-phonon coupling analogously to what has been found to drive superconductivity in MgB_2 , and present evidence that at hole-doping levels similar to that reported, the hole – bond-stretch coupling is surprisingly strong and makes phonon exchange a prime candidate for the mechanism of pairing. In the case that such coupling is strong, it can be verified by spectroscopy of the Raman-active bond stretch mode. In fact, Ekimov *et al.* report [4] a Raman spectrum in which the sharp diamond peak at 1332 cm^{-1} has vanished, leaving spectral weight in the $1000\text{-}1300 \text{ cm}^{-1}$ range. This behavior is a plausible extrapolation (considering they are very differently prepared materials) from more lightly B-doped films in which Ager *et al.* observed an initial weakening and broadening of the

1332 cm^{-1} mode,[15] and a transfer of spectral density to peaks in the 940-980 cm^{-1} range for concentrations $\sim c_{sc}$. Zhang *et al.* reported, for films with concentration $\sim \frac{1}{3}c_{sc}$ a broad peak at 1200 cm^{-3} and a very broad feature peaking at 485 cm^{-3} . [16]

For the sake of definiteness, we consider a hole concentration of 0.025/carbon atom, 10% less than the B concentration (c_{sc}) determined for the superconducting diamond films. At this concentration the hole Fermi energy E_F lies 0.61 eV below the valence band maximum, and the diamond Fermi surfaces consist of three zone-centered “spheroids.” The outer one in particular differs considerably from spherical due to the anisotropy of the band mass, but effects of anisotropy will be decreased by disorder scattering and in any case would give only second order corrections to the properties that we calculate.

The system we consider is thus 2.5% hole-doped diamond. The key points here are (1) the carrier states are the *very strongly* covalent bonding states that make diamond so hard, and (2) these states should be sensitively coupled to the bond-stretching mode, which lies at the very high frequency of 1332 cm^{-1} (0.16 eV) in diamond. These ingredients are the same as those prevailing in MgB_2 . There are differences, both of a positive and negative nature. In MgB_2 only two of the nine phonon branches are bond-stretching, whereas in diamond these comprise three of the six branches. On the other hand, MgB_2 is strongly two dimensional in its important bands (σ bands), which means a near-step-function increase in the density of participating states as doping occurs; the states in diamond are three-dimensional and their Fermi level density of state $N(0)$ increases with doping level more slowly.

A look at the phonon spectrum of diamond[17] reveals that the three optic modes are the bond stretching ones, and they have little dispersion so $\bar{\Omega}_o \approx 0.15$ eV is their common unrenormalized frequency. The theory of carrier-phonon coupling and the resulting superconductivity in such systems is well developed, and the important features in MgB_2 -like systems have been laid out explicitly. The coupling strength λ is given rigorously for an element by

$$\lambda = \frac{\sum_b N_b(0) \langle I_b^2 \rangle}{M \langle \omega^2 \rangle} = \frac{N(0) I_{rms}^2}{M \omega_o^2} \quad (1)$$

where $N_b(0)$ is the DOS of band b , M is the carbon mass, $I_b^2 \equiv \langle |I_b(k, k')|^2 \rangle_{FS}$ is the Fermi surface averaged electron-ion matrix element squared for band b , and $\langle \omega^2 \rangle$ is an appropriately defined mean square frequency which will simplify to ω_o^2 , the bond stretch frequency renormalized by the hole doping. The sum over bands b has been displayed explicitly but finally leads to an rms electron-ion ma-

trix element in the numerator, and the Fermi level density of states is $N(0)=0.060$ states/eV per cell per spin.

Due to non-sphericity and non-parabolicity of the three inequivalent bands substantial computation would be required to obtain accurate numbers (and anharmonic and non-adiabatic corrections would change them, see below). There are two ways to obtain approximate values in a pedagogical manner: (1) calculate the $Q=0$ deformation potentials to obtain the matrix elements for the optic modes, or (2) calculate the phonon softening and use the lattice dynamical result

$$\begin{aligned} \omega_Q^2 &= \Omega_Q^2 + 2\Omega_Q \text{Re} \Pi(Q, 0) \\ \omega_o^2 = \omega_{Q \rightarrow 0}^2 &\rightarrow \Omega_o^2 - 2\Omega_o N(0) |\mathcal{M}|^2. \end{aligned} \quad (2)$$

where $\Pi(Q, \omega)$ is the phonon self energy arising from the doped holes, and \mathcal{M} is the electron-phonon matrix element and is determined by I_{rms} (see below). We apply both methods to obtain estimates of the coupling strength.

The calculations were done with the Wien2k linearized augmented plane wave code.[18] The basis size was fixed by $R_{mt}K_{max} = 7.0$ with a sphere radius 1.2 for all calculations. While 110 irreducible \mathbf{k} points were used for pure diamond, 1156 \mathbf{k} points in the irreducible wedge for the B-doped diamond virtual crystal calculations, (nuclear charge $Z = (1-x)Z_C + xZ_B = 5.975$) because the Fermi surface volume had to be sampled properly to account for screening. Alloy (coherent potential approximation, CPA) calculations using the full potential local orbital code[19] give bands as in our virtual crystal model, the main difference[20] being small disorder broadening that would not change our conclusions.

The central quantity in Eq. 1 is the matrix element, which can be expressed in terms of the deformation potential \mathcal{D} ; we use the definitions of Khan and Allen[21] to avoid ambiguity. \mathcal{D} is the shift in the hole (valence) band edge with respect to the bond stretching motion, whose scale is given by $u_o = \sqrt{\hbar/2M\Omega_o} = 0.034$ Å. The stretching mode is threefold degenerate and can have any direction of polarization. We have chosen the polarization in which atoms move along a $\langle 111 \rangle$ direction. Under this displacement, the threefold eigenvalue splits (see Fig. 1 for the case of doped diamond) at the rate of $\Delta(\epsilon_{upper} - \epsilon_{lower})_{k=0}/\Delta d_{bond} = 21$ eV/Å, where d_{bond} is the bond length. Since the twofold band splits half as rapidly as the single band (and oppositely) this leads to the two deformation potentials of magnitude $\mathcal{D}_1 = 14$ eV/Å for the nondegenerate band and $\mathcal{D}_2 = 7$ eV/Å for the doublet, for intrinsic diamond. The large deformation potential is 60% larger than the (already large) analogous one in MgB_2 .

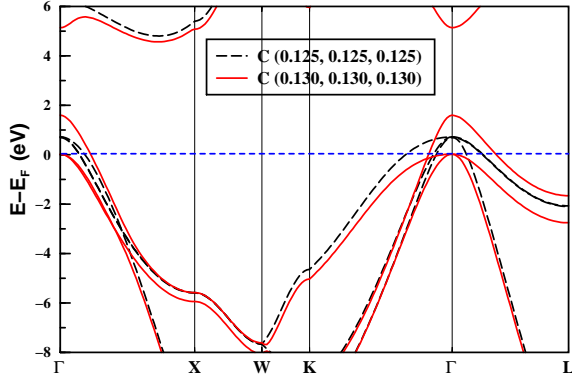


FIG. 1: (Color online) Virtual crystal bands of 2.5% B-doped diamond without (dashed lines) and with (solid lines) a bond stretch phonon frozen in. The atomic displacement $a\sqrt{3}\Delta x = 0.0309 \text{ \AA}$ is just enough to transfer all holes to within a single $k=0$ centered Fermi surface. The horizontal dashed line indicates the Fermi level (aligned for this plot). X denotes the usual zone boundary point, L designates the zone boundary point in the $\langle 111 \rangle$ direction parallel to the atomic displacements.

The results for 2.5% B-doping are needed for calculation of the coupling strength, and are shown in Fig. 1. They are renormalized by B-doping by 3% (downward) from those of intrinsic diamond, so again we have $\mathcal{D}_1 = 14 \text{ eV/\AA}$, $\mathcal{D}_2 = 7.0 \text{ eV/\AA}$. These deformation potentials are undoubtedly the largest yet encountered for any metallic solid, being directly related to the great bond strength of diamond. Since the three deformation potentials contribute additively to the coupling strength, we simplify by using the root mean square value $I_{rms} = 10 \text{ eV/\AA}$. The rms electron-phonon matrix element, to be used below, is $\mathcal{M} = \sqrt{\omega_o/\Omega_o} u_o I_{rms} = 0.70 \text{ eV}$; here ω_o is the renormalized optic frequency.

Together with the value $N(0) = 0.060 \text{ states/eV-spin}$, $M\Omega_o^2 = 65 \text{ eV/\AA}^2$, and (calculated below) $\omega_o^2 = 0.68\Omega_o^2$, we obtain from Eq. 1 the coupling strength $\lambda = 0.55$. The coupling is confined to a set of three optic branches which comprise a narrow peak centered at ω_o . The conventional theory, neglecting very minor strong-coupling corrections,[22] gives $T_c = (\omega_o/1.2) \exp[-1/(\frac{\lambda}{1+\lambda} - \mu^*)]$, where μ^* is an effective Coulomb repulsion that is uncertain for doped diamond. Using the conventional value $\mu^* = 0.15$ with $\omega_o = 0.128 \text{ eV}$ gives $T_c = 9 \text{ K}$, gratifyingly (and probably fortuitously) close to the experimental values of 4 K to 7 K. To obtain the initially observed value $T_c = 4 \text{ K}$ would require $\lambda = 0.48$, or alternatively $\mu^* \approx 0.20$, *i.e.* relatively small changes.

A less direct way of obtaining the coupling strength, but one that (numerically) includes averaging over bands properly, is to calculate the renormalized phonon frequency and apply Eq. 2. The calcu-

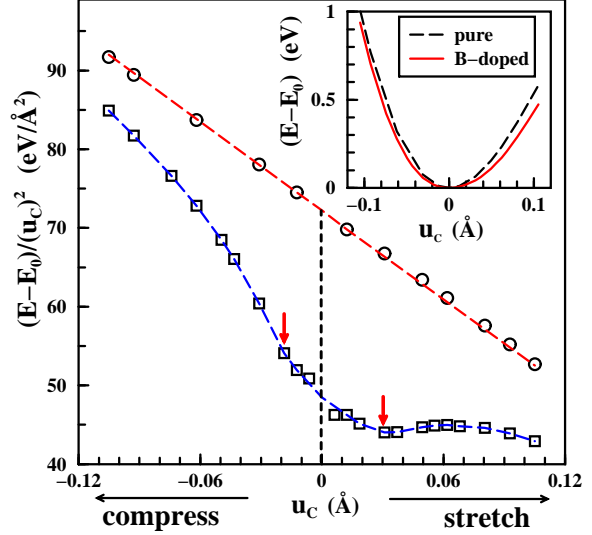


FIG. 2: (Color online) Plots of the energy of distortion for the frozen-in bond stretch mode, for (top straight line) undoped diamond, and (bottom line) 2.5% B-doped diamond. The coordinate u_C is for one of the two identically displaced atoms. Pristine diamond follows a quadratic plus lowest-order anharmonic form $\Delta E(u) = A_2 u^2 + A_3 u^3$ accurately, as indicated by the straight dashed line. After doping the $\Delta E(u)$ functional form becomes very complex. The horizontal arrows indicate the atomic displacements for which one (or two) Fermi surfaces disappear. The inset shows the $\Delta E(u)$ curves themselves.

lated change in energy versus atomic displacement, plotted as $\Delta E(u)/u^2$, is shown in Fig. 2, both for intrinsic and doped diamond. The difference due to doping is striking. The result for diamond is simple to understand: the harmonic u^2 term gives $\Omega_{harm} = 1308 \text{ cm}^{-1}$ similar to literature values,[17, 23] and the $A_3 u^3$ term quantifies its anharmonicity.

The $\Delta E(u)/u^2$ curve for the doped case (see Fig. 2) is much more complex. The reason is clarified by the red arrows on the plot, which mark the displacements where some piece(s) of Fermi surface vanishes. One of these values of displacement is also used for the deformation potential plot of Fig. 1, where one shifted band edge is lying exactly at E_F . Boeri *et al.* have described how, at such topological transitions of the Fermi surface, the energy is non-analytic.[24] In Fig. 2 one can imagine a straight line behavior similar to (and nearly parallel to) that of diamond for u_C between the two topological transitions, with changes of behavior occurring beyond each transition point. It is of special relevance that these positions are roughly at the bond-stretch amplitude, hence they are physically important.

Returning to the coefficient of the u^2 (harmonic) term, for the doped case it is 0.68 that of diamond,

giving (in harmonic approximation) $\omega_o = 1070 \text{ cm}^{-1}$. This renormalization of the square of the optic mode frequency (see Eq. 2) by 32% is a vivid indication of the strong coupling, even for the case of 2.5% holes. Substituting ω_o ratio into Eq. 2 allows us to extract the electron-phonon matrix element $\mathcal{M} = 0.67 \text{ eV}$, within 5% of the value obtained from the deformation calculation. Combined with the deformation potential result, the predicted coupling strength is $\lambda = 0.53 \pm 0.03$. As mentioned above, this value is quite consistent with the observed critical temperature, but certainly such good agreement may not be warranted.

Our treatment neglects some complicating features. The Jahn-Teller splitting of the isolated B substitutional impurity (0.8 cm^{-1} from Fabry-Pérot spectroscopy[25]) is three orders of magnitude smaller than energy differences involved in the bond-stretch mode and therefore is negligible. It has been suggested[12, 13] that supercells offer a more realistic model than a virtual crystal treatment. Our calculation of a C_{31}B supercell indicated strong ordered-boron effects (which are unphysical), and our CPA alloy calculations[20] give bands like the virtual crystal model, with small disorder broadening added. Another factor is anharmonicity, which includes conventional anharmonicity and the non-adiabatic effects that cause the non-linearity of $\Delta E(u)/u^2$ in Fig. 2. Making the anharmonic corrections need not change the effective phonon frequency greatly, as shown for MgB_2 by Lazzeri *et al.*[26] who found that for MgB_2 three- and four-phonon corrections gave strongly canceling corrections to the vibrational frequency. The valid-

ity of the Migdal-Eliashberg itself becomes an interesting question, and more so for lower doping levels. For the 2.5% concentration considered here, the ratio of phonon frequency to electron energy scales is $\omega/E_F = 0.25$, certainly not the small parameter that is usually envisioned as a perturbation expansion parameter. Doped diamond provides a new system in which to investigate non-adiabatic effects.

Now we summarize. Based on the experimental information available so far, the B doping level in diamond achieved by Ekimov *et al.* should result in hole doping of the diamond valence bands to a level $E_F \approx 0.6 \text{ eV}$. Calculations bear out the analogy to MgB_2 that deformation potentials due to bond stretching are extremely large, and evaluation of the hole-phonon coupling strength using conventional theory leads to $\lambda \approx 0.55$, a renormalization of the optic mode frequency by -20%, and T_c in the 5-10 K range. These results indicate that phonon coupling is the likely candidate for the pairing mechanism, consistent with the conclusions of Boeri *et al.*[11] The low carrier density (for a metal) implies both poor screening of the Coulomb interaction and the intrusion of non-adiabatic effects, which are primary candidates for further study. Higher doping levels should increase T_c , but probably not to anything like that occurring in MgB_2 . Definitive calculations will require CPA calculations of the electron-phonon coupling characteristics.

The authors acknowledge Z. Fisk for pointing out Ref.[4], and J. Kuneš and K. Koepernik for technical advice and J. Kuneš for a critical reading of the manuscript. This work was supported by National Science Foundation Grant DMR-0114818.

-
- [1] J. Nagamitsu *et al.*, Nature **410**, 63 (2001).
 - [2] J.M. An and W.E. Pickett, Phys. Rev. Lett. **86**, 4366 (2001); J. Kortus *et al.* Phys. Rev. Lett. **86**, 4656 (2001); Y. Kong *et al.*, Phys. Rev. B **64**, 020501 (2001); T. Yildirim *et al.*, Phys. Rev. Lett. **87**, 037001 (2001); H. J. Choi *et al.*, Physica C **385**, 66 (2003); W. E. Pickett *et al.*, Physica C **328**, 1 (2003).
 - [3] See J. An and W. E. Pickett, Ref. [2].
 - [4] E. A. Ekimov *et al.*, Nature **428**, 542 (2004).
 - [5] Y. Takano *et al.*, cond-mat/0406053.
 - [6] S. A. Kajihara *et al.* Physica B **185**, 144 (1993); Phys. Rev. Lett. **66**, 2010 (1991).
 - [7] S. J. Breuer and P. R. Briddon, Phys. Rev. B **49**, 10332 (1994).
 - [8] For a recent overview, see K. Thonke, Semicond. Sci. Technol. **18**, S20 (2003).
 - [9] R. F. Mamin and T. Inushima, Phys. Rev. B **63**, 033201 (2001)
 - [10] F. Fontaine, J. Appl. Phys. **85**, 1409 (1999).
 - [11] L. Boeri, J. Kortus, and O. K. Andersen, cond-mat/0404447.
 - [12] H. J. Xiang *et al.*, cond-mat/0406644.
 - [13] X. Blase *et al.*, cond-mat/0407604.
 - [14] G. Baskaran, cond-mat/0404286.
 - [15] J. W. Ager III *et al.*, Appl. Phys. Lett. **66**, 616 (1995).
 - [16] R. J. Zhang, S. T. Lee, and Y. W. Lam, Diamond Rel. Mater. **5**, 1288 (1996).
 - [17] P. Pavone *et al.*, Phys. Rev. B **48**, 3156 (1993).
 - [18] WIEN97: see P. Blaha, K. Schwarz, and J. Luitz, Vienna University of Technology, 1997, improved and updated version of the original copyrighted WIEN code, which was published by P. Blaha, K. Schwarz, P. Sorantin, and S. B. Trickey, Comput. Phys. Commun. **59**, 399 (1990).
 - [19] <http://www.ifw-dresden.de/agtheo/FPLO/>
 - [20] K.-W. Lee and W. E. Pickett, unpublished.
 - [21] F. S. Khan and P. B. Allen, Phys. Rev. B **29**, 3341 (1984); P. B. Allen, in *Dynamical Properties*

- of Solids*, ed. G. K. Horton and A. A. Maradudin (North-Holland, Amsterdam, 1980), Ch. 2.
- [22] P. B. Allen and R. C. Dynes, *Phys. Rev. B* **12**, 905 (1975).
- [23] M. J. Mehl and W. E. Pickett, in *Raman Scattering, Luminescence and Spectroscopic Instrumentation in Technology*, Proc. SPIE **1055**, eds. F. Adar, J. E. Griffiths and J. M. Lerner (SPIE, Bellingham, Wash., 1989), pp. 181-184.
- [24] L. Boeri *et al.*, *Phys. Rev. B* **65**, 214501 (2002).
- [25] H. Kim *et al.*, *Phys. Rev. Lett.* **83**, 4140 (1999).
- [26] M. Lazzeri, M. Calandra, and F. Mauri, *Phys. Rev. B* **68**, 220509 (2003).